CHEMISTRY OF MATERIALS

Article

pubs.acs.org/cm

Revisiting the Anion Framework Conservation in Cation Exchange Processes

Noga Meir,[†] Beatriz Martín-García,[‡] Iwan Moreels,[‡] and Dan Oron*[,†,§]

[†]Department of Physics of Complex Systems, Weizmann Institute of Science, Rehovot 7610001, Israel

[‡]Nanochemistry Department, Istituto Italiano di Technologia, Via Morego 30, IT-16163 Genova, Italy

Supporting Information

ABSTRACT: We investigated the effect of cation exchange on the anionic framework of lightly doped CdSe:Te/CdS nanorods. In contrast with previously studied core/shell systems, the Te dopant, located in the center of the CdSe core, provides an extremely sensitive indicator for any structural changes of the anionic framework that may occur as a result of the cation exchange process. We first optimized the cation exchange procedure in order to retain the fluorescence properties of the CdSe:Te/CdS nanorods after exchange of Cd^{2+} for Cu^{+} and back to Cd^{2+}. Next, using multiexciton spectroscopy, we were able to probe the magnitude of the exciton−exciton repulsion interaction and use that to assess the degree of crystal structure conservation. Our findings provide a much stronger proof that the anion framework is indeed rigid, showing no evidence of significant migration of the anionic dopant.

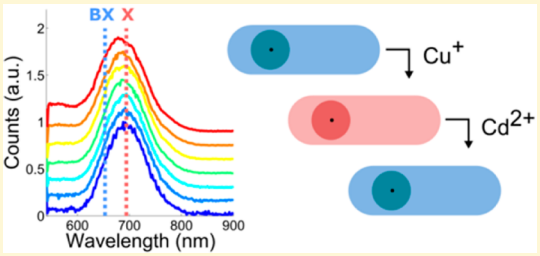

INTRODUCTION

The process of cation exchange in semiconducting nanocrystals has been in use for many years as an important synthetic tool to access a variety of chemical and crystallographic phase nanocrystals which are not easily accessed by hot-injection methods. In recent years a variety of reversible,[1,2] sequential,[3,4] and partial[5−10] cation exchange techniques were demonstrated in quantum dots (QDs). The relative simplicity with which one can perform cation exchange, as well as the excellent conservation of the overall crystal structure achieved in many cases, are just some of the advantages of using cation exchange for the purpose of synthesizing novel nanomaterials.

However, insufficient attention was given to the possible effect cation exchange processes can have on the anionic framework of the crystal. Although this issue was addressed by examination of a cyclic cation exchange performed on the extensively studied CdSe/CdS dot-in-rod system,[11] the spectroscopic tools used for this end—namely, linear absorption and photoluminescence spectroscopy—were not sensitive enough to account for subtle changes of the anionic crystal structure, both in the core and in the vicinity of the core/shell interface. More recent work on cation exchange from Cu_2Te to CdTe nanodisks[12] did reveal that displacements in the anion sublattice can lead to a reconstruction of the crystal. However, it required detailed investigation of the samples using high resolution transmission electron microscopy to reveal the changes—a method which is difficult to implement when contrast between different atoms in the lattice is poor.

In this study we propose to spectroscopically investigate the effect of cation exchange using a modified version of the CdSe/CdS nanorods (NRs). These nanorods' CdSe cores are very lightly doped with only one or a few atoms of Te, located at the center of the CdSe core via nucleation doping (Figure 1). Upon excitation, a hole from the top of the CdSe host valence band

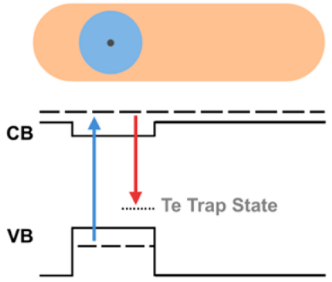

Figure 1. Schematic illustration of the structure and band alignment for Te-doped CdSe/CdS nanorods.

undergoes fast nonradiative relaxation to the Te trap state, leading to a relatively large Stokes shift compared to undoped CdSe QDs.[13−15] Upon further excitation of these QDs, the strong localization of the hole wave function around the Te dopant evokes a significant Coulombic hole−hole repulsion, resulting in a large blue-shift of the biexciton (BX) relative to the single exciton.[14,13] Unlike most emission properties (and specifically the band-edge emission color), the magnitude of the exciton−exciton interaction strongly depends on the position of the Te dopants within the nanocrystal.[15] This provides us with a unique and highly sensitive spectroscopic handle through which we can identify whether Te dopants have diffused toward

Received: August 15, 2016
Revised: October 13, 2016
Published: October 13, 2016

DOI: 10.1021/acs.chemmater.6b03332
Chem. Mater. 2016, 28, 7872−7877

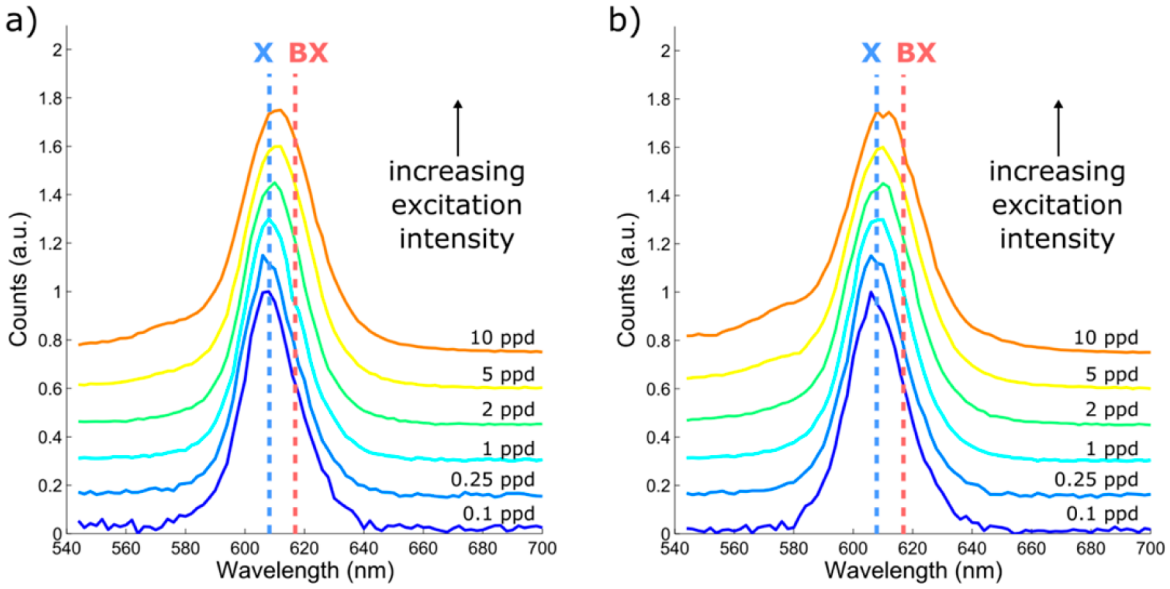

Figure 2. Emission spectra at increasing excitation intensities, ranging from 0.1 ppd (photon per dot) to 10 ppd, of CdSe/CdS NRs (a) before and (b) after the cation exchange. Locations of the X and BX centers were extracted from the numerical fit. In both cases, the BX red-shift is ∼30 meV.

the edges of the nanocrystal as a result of the cation exchange process. Exciting these NRs with increasingly higher photon fluences allowed us to detect the emission emanating from the biexcitons and extract the BX binding (or repulsion) energy, in order to determine if any alteration of the anionic framework has occurred.

RESULTS AND DISCUSSION

We first establish the use of multiexciton spectroscopy in the context of cation exchange processes by reproducing the results presented in ref 11 for CdSe/CdS NRs and further expanding our insight regarding the multiexcitonic behavior of this system. CdSe/CdS NRs were synthesized with a core diameter of 3.6 nm and were then subjected to a cyclic cation exchange process, replacing Cd^{2+} cations with Cu^{+} and then back to Cd^{2+}. To maintain the overall structure and maximize the recovery of the initial optical properties, which is essential for the following spectroscopic studies, we used a similar $Cd^{2+} \rightarrow Cu^{+}$ exchange as proposed by Jain et al.,[1] while further adapting the subsequent $Cu^{+} \rightarrow Cd^{2+}$ step to improve photoluminescence. The approach here proposed relies on the use of cadmium acetate dissolved in oleylamine as precursor, and a repetition of the $Cu^{+} \rightarrow Cd^{2+}$ exchange step, at 250 °C. This follows the recent results of Li et al. on cation exchange at elevated temperature to produce highly fluorescent ZnSe/ZnS nanorods[16] and CdTe nanodisks[12] and is adopted to minimize defects and Cu impurities already during the cation exchange, avoiding the need for postsynthesis annealing procedures.[1] The linear emission spectra, more specifically the emission wavelength of the NRs and the emission peak full-width at half-maximum (fwhm), did not change as a result of the cation exchange (Supporting Information, Figure S1). The increasing PL QY after each exchange step is in line with reduced Cu concentration observed with elemental analysis (Supporting Information, Table S1). Finally, after three $Cu^{+} \rightarrow Cd^{2+}$ exchange steps we obtained a recovery of 68% of the initial QY value, demonstrating the efficiency of our procedure.

Examination of the multiexcitonic properties of these NRs was performed in order to ascertain the nature of the exciton−exciton (X−X) interaction. These measurements also serve as a control experiment for the main section of this manuscript, investigating the effect of cation exchange using Te-doped CdSe/CdS NRs. A dilute solution of the NRs dispersed in toluene was excited by a 5 ns pulsed laser at 450 nm and increasing intensities, reaching excitation levels as high as 10 photons/QD on average for each excitation pulse (details regarding the calculation of the amount of photons/dot can be found in the Supporting Information). Time-resolved fluorescence signals were filtered through a monochromator and then collected by a photomultiplier tube, at wavelengths ranging from 540 to 700 nm. These were then integrated around the peak of the excitation pulse to construct the transient emission spectrum as a function of the (increasing) excitation intensity. Figure 2 presents the constructed emission spectra of the CdSe/CdS NRs, before and after the cation exchange. In order to resolve the biexcitonic (BX) feature, the emission spectrum at low excitation intensity was used to determine the emission line shape of the singly excited dots, followed by a numerical global fit of the three highest intensity spectra to a sum of three spectral components. More details regarding the BX analysis are presented in the work of Banin and co-workers[17] and in the Supporting Information.

For both samples we observe a red-shift of the main emission peak and the emergence of a blue-shifted shoulder at increasing excitation intensities. The former is associated with the BX emission whereas the latter is due to emission from higher excited states. The nature of the exciton−exciton interaction in this system is known to be dependent on the dimensions of the core, which can lead to either type-I or quasi-type-II behavior due to changes in the extent of electron delocalization.[18] In this particular case, we should expect an attractive interaction, and indeed we observed a red-shift of the BX of ∼30 meV, both before and after the cation exchange. The nature and magnitude of the exciton−exciton interaction are both in accordance with previously published results.[18]

We now turn to discuss our findings regarding the spectroscopic examination of the Te-doped NRs. Te-doped CdSe QD cores were synthesized in three different sizes and

DOI: 10.1021/acs.chemmater.6b03332
Chem. Mater. 2016, 28, 7872−7877

later overcoated with rod-like CdS shells. These will be referred throughout the rest of this manuscript as small-, medium- and large-core samples, with respective core diameters of 2.6 nm, 3.6 nm, and 4.2 nm. All three types of Te-doped nanorods were also subjected to the cyclic cation exchange, under the same conditions used for the undoped CdSe/CdS NRs.

Standard optical characterization of a typical medium-core NR sample is presented in Figure 3, showing the linear

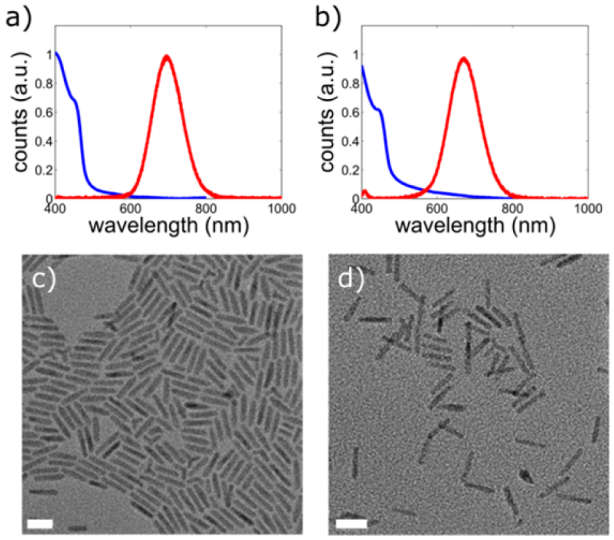

Figure 3. (a, b) Absorption (blue) and emission (red) spectra of the medium-core NRs, before (a) and after (b) the cyclic cation exchange. Emission peaks appear at 696 nm (a) and 671 nm (b). (c, d) TEM images of the same nanorods presented in a and b, before (c) and after (d) cation exchange. Scale bar is 20 nm.

absorption and emission spectra before and after the cation exchange (Figure 3a,b, respectively). Comparing these two emission spectra, we see no new excitonic features, as well as conservation of the PL bandwidth (fwhm is ∼100 nm, characteristic of emission associated with the Te dopant), indicating no change in the sample size distribution occurred. However, in contrast with the undoped samples, there is a noticeable blue-shift of the emission peak after the cation exchange, which appeared in all samples of the Te-doped NRs examined, for all three core sizes (note that to some extent such a shift was observed also in ref 11). Generally speaking, such a blue-shift can be attributed to a decrease either in the core diameter or in the shell thickness. A change in the effective core diameter in a dot-in-rod system can occur as a result of alloying around the core/shell interface. However, Klimov and co-workers have already shown that for CdSe/CdS core/shell QDs, the emission blue-shift resulting from alloying in the core/shell interface was significantly lower than in our case, even when a considerable portion of the interface was alloyed.[19]

TEM data showed that the emission blue-shift is likely due to etching of the CdS shell. Analyzing the sizes of ∼100 NRs from TEM micrographs of this sample, both before and after the cation exchange (typical TEM images shown in Figure 3c,d), showed a decrease of ∼0.8 nm in the NR diameter. Assuming the core diameter remained unaltered, this changes the thickness of the CdS shell in the radial direction from ∼0.7 nm to ∼0.3 nm, equivalent to a decrease from two monolayers (MLs) of wurtzite CdS to only one. In previous studies, in which core/shell CdSe/CdS QDs were synthesized with a core diameter similar to that in our case and with a thin CdS shell at various thicknesses,[20,21] the difference in the emission wavelength resulting from decreasing the shell thickness from 2 to 1 ML is comparable with the emission blue-shift measured here (∼66 meV), strengthening our conclusion linking the emission blue-shift to etching of the CdS shell. The fact that this etching was not observed for the undoped CdSe/CdS NRs is reasonable considering the different synthetic procedures used to fabricate the doped and undoped CdSe cores and the presence of different organic ligands used to passivate the cores prior to the NR seeded growth. These can potentially lead to a different surface chemistry that can affect the subsequent shell growth and finally the cation exchange process, even though similar synthetic procedures were used for the CdS shell growth. Despite the small etching, the cation exchange did not significantly reduce the PL QY, as final values for the three types of NRs reach approximately 80% of the initial PL QY. Note that the slight decrease is more consistent with reducing the thickness of a thin passivating CdS layer[20,22] and less typical for alloying in the core/shell interface.[19] The QY values and their standard deviations are presented in Table 1.

Table 1. Average QY Values Measured before and after the Cation Exchange

	before CE	after CE	QY recovery
small cores	69 ± 3%	60 ± 3%	87%
medium cores	76 ± 1%	64 ± 5%	84%
large cores	86 ± 1%	63 ± 6%	74%

As stated before, the linear absorption and emission spectroscopy, while corroborating the work of Jain et al.,[11] do not yet provide a definite proof for full conservation of the anionic framework in these QDs. Indeed, as was shown by Franceschetti and co-workers,[15] the Stokes shift due to the Te dopant is quite insensitive to the dopant position. This calls for a more sensitive technique such as BX spectroscopy to verify the absence of changes in the anion framework. Measuring the BX properties of the Te-doped NRs was conducted in the same manner described before for the undoped CdSe/CdS NRs. Figure 4 presents typical emission spectra for a medium-core sample, taken at increasing excitation intensities, before and after the cation exchange. Here, the photon fluence of the excitation beam reached excitation levels as high as 15 ppd, and the fluorescence transients were recorded from 540 to 900 nm. Similarly to the undoped CdSe/CdS NRs, we can see the development of the BX feature with the increase of photon fluence. In this case, however, it is reflected as a blue-shift of the main emission peak due to the repulsive nature of the X−X interaction. Also detectable is an additional feature around ∼550 nm. This short-lived feature appeared in all measurements performed for the Te-doped NRs and is attributed to surface-trap emission from the CdS, which was also taken into account in the analysis. Notably, all of the Te-doped NRs exhibited a noticeable blue-shift of the BX emission, even after the cation exchange process.

We performed the BX spectroscopy measurements for all three core sizes. For each core size we measured several cation-exchanged samples, as we have noticed that in the case of the doped cores post-cation exchange, samples are more prone to experience some damage, likely due to the surface modification. To avoid the possibility of sample degradation, the NRs were measured as close as possible to the time of the cation

DOI: 10.1021/acs.chemmater.6b03332
Chem. Mater. 2016, 28, 7872−7877

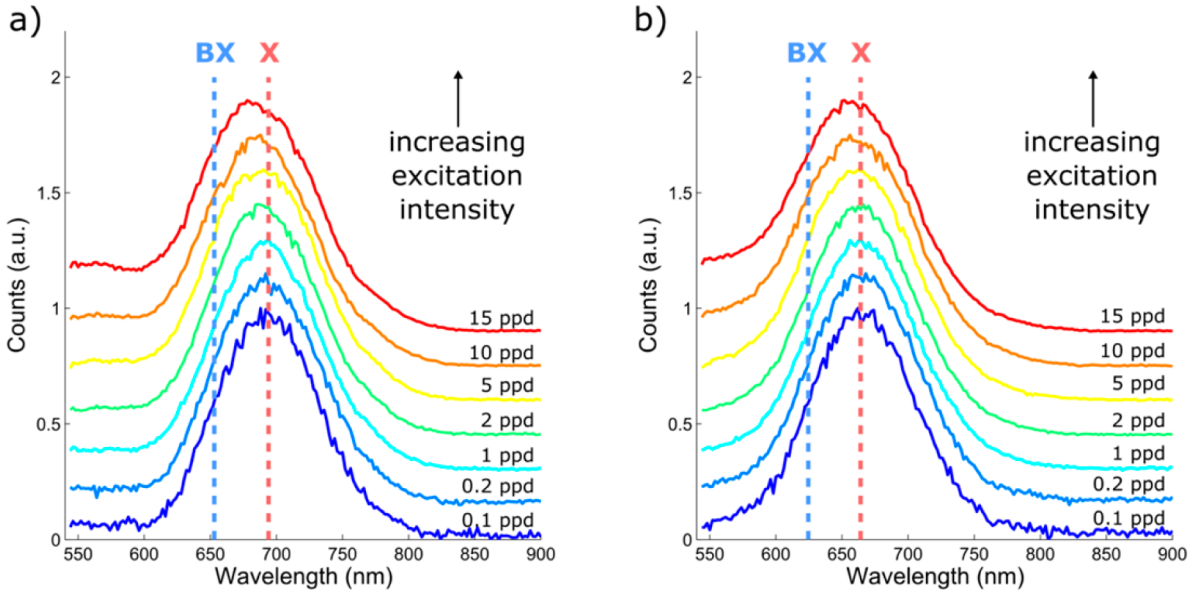

Figure 4. Emission spectra at increasing excitation intensities, ranging from 0.1 ppd (photon per dot) to 15 ppd, presented for a typical medium-core sample of CdSe:Te/CdS NRs, (a) before and (b) after the cation exchange (the same sample presented in Figure 3). Locations of the X and BX centers were extracted from the numerical fit.

exchange, and in the meantime they were stored under inert atmosphere. For each measurement the BX emission peak was extracted and the energy difference between the X and the BX (here referred to as "BX shift") was plotted against the emission wavelength of the same sample. This plot is presented in Figure 5. Two cation-exchanged NR samples exhibited significant deviation from the measured trend, as well as considerably lower QY compared to other samples with the same dimensions. Therefore, the data points corresponding with these samples were redacted from this plot. The corresponding plot, including the redacted data points, appears in the Supporting Information.

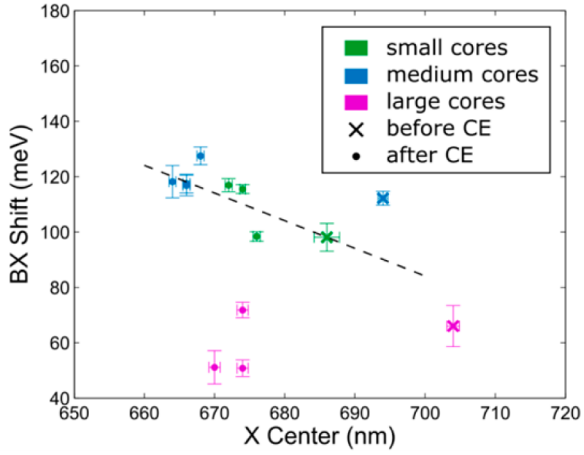

Figure 5. BX shift values plotted against X peak for all the NRs samples measured. Small, medium, and large core samples are labeled in green, blue, and purple, correspondingly. The expected trend for the change of the BX shift with the X center for the small core sample (−1 meV/nm) is marked with a dashed line.

If the anion framework is maintained, one would expect to see a similar BX shift before and after cation exchange, while migration of Te ions would be reflected in a lower BX shift. This is due to the fact that as the Te impurity moves away from the CdSe center, the hole wave function becomes more shallow and less localized around the Te inclusion, thus reducing the BX repulsion.[15] For example, for ∼1 nm migration of the Te impurity from the center of the CdSe core, we should expect a decrease of the BX repulsion of ∼50 meV.[15] Looking at Figure 5, it is clear that the BX shift in the cation exchanged samples is either equal to or higher than its value before cation exchange. The increase in BX shift appears to be surprising at first. Since, however, for all three core sizes we can see a blue-shift of the singly excited dot emission after the cation exchange, we need to also take into account its secondary effect on the BX shift.

Examining in detail the trend exhibited by each of the core sizes, we detect little to no change of the BX shift following cation exchange for the large and medium cores and a small increase for the small cores. The trend of the BX shift with the emission wavelength for the small-cores samples is very close to −1 meV/nm (as labeled with a dashed line in Figure 5). This is consistent with the change of the BX shift with shell thickness in Te-doped core/shell CdSe/CdS, which has already been experimentally characterized for this core size.[14] From simple effective mass considerations this slope should be smaller for larger cores, where the degree of carrier delocalization into the shell is smaller.

Overall, based on the results presented in Figure 5, we can therefore determine that the X−X interaction was unaltered after the cation exchange process for all core sizes. The work of Franceschetti and co-workers[15] clearly showed that any change in the position of the Te dopants from the center of the CdSe host, whether it is a migration of a single Te atom toward the edges of the nanocrystal or a diffusion of more than one dopant to form a somewhat "random" distribution of the few Te atoms across the CdSe core, will result in a significant decrease of the magnitude of the hole−hole repulsive interaction and therefore of the BX shift as well. Thus, the BX shift measurements not only provide further confirmation for the etching of the CdS shell after the cation exchange, but more importantly, they

DOI: 10.1021/acs.chemmater.6b03332
Chem. Mater. 2016, 28, 7872−7877

verify the validity of the claims regarding the extreme rigidity of the anionic framework.

CONCLUSIONS

We used multiexciton spectroscopy of lightly doped CdSe:Te/CdS nanorods, which underwent a cyclic cation exchange, in order to evaluate the influence of such process on their anionic crystal structure. Although the optical properties of the NRs measured before and after the cation exchange indicated some structural change, we could attribute this to surface effects as the modifications resulted from a slight etching of the outer CdS shell. Analysis of the emission related to biexcitons revealed that the Te dopants, whose location is strongly dependent on the X−X interaction, did not diffuse within the crystal. Therefore, we conclude that the anionic framework of the NRs was not altered by the cation exchange process.

Unlike other methods formerly employed to detect subtle changes in the crystal structure of QDs, such as high-resolution electron microscopy, multiexciton spectroscopy is far simpler to execute and does not require individual probing of each isolated QD. Furthermore, multiexciton spectroscopy can be employed to measure other QD properties which can be highly sensitive to ion migration (such as multiexciton Auger lifetimes), potentially providing a more general method for evaluating lattice conservation, even without the need for doping.

METHODS

Synthesis. *Te-Doped CdSe Cores Synthesis.* A total of 52 mg CdO, 240 mg of TDPA, and 20 mL of ODE were degassed in a 50 mL flask under vacuum at 120 °C for 30 min. The temperature was raised to 290 °C under argon flow, and a mixture of 2 mL Se:TOP (0.1 M) and 120 μL Te:TOP (0.1 M) solutions was injected into the flask. The reaction was stopped after 10 s−3 min. A total of 2 mL of nonanoic acid were added upon cooling (at ∼100 °C).

CdSe Cores Synthesis. A total of 60 mg CdO, 280 mg of ODPA, and 3 g of TOPO were degassed in a 50 mL flask under vacuum at 120 °C for 30 min. The temperature was then raised to 380 °C under Ar flow. At ∼ 340 °C the CdO started to dissolve, and 1.8 mL of TOP was injected. At 380 °C, a solution containing 58 mg of Se in 0.5 mL of TOP was quickly injected into the flask, and the heating was removed immediately.

CdSe:Te/CdS or CdSe/CdS Rod Synthesis. Purified CdSe:Te dots were used as cores for the seeded-growth of CdS nanorods. A total of 64 mg CdO, 312 mg of ODPA, 82 mg of HPA, and 3 g of TOPO were degassed in a 50 mL flask under vacuum at 150 °C for 1 h. The temperature was raised to 350 °C under argon flow, and 2 mL of TOP were added upon dissolution of the CdO. At 350 °C, a solution of 120 mg of S in 2 mL of TOP, mixed with 1 mL of CdSe:Te or CdSe in TOP, was injected to the flask. The amounts of core dots used for the synthesis of the small, medium, and large-core Te-doped NRs were 53, 35, and 15 mmol, respectively. The amount of core dots used for the undoped NRs was 60 mmol. The reaction was stopped after 2−3 min. A total of 2 mL of nonanoic acid was added upon cooling (at ∼100 °C).

Cation Exchange. Both steps of the cation exchange were performed in an air- and moisture-free glovebox. For the $Cd^{2+} \rightarrow Cu^{+}$ exchange, 2 mL of a NR solution in toluene was taken with $[Cd^{2+}]$ = 1 mM. The Cd^{2+} concentration was determined by the CdSe/CdS absorbance at 295 nm, using the absorption coefficient of Angeloni et al.[23] (see Supporting Information). Under vigorous stirring, 1 mL of a solution containing 30 mg of tetrakis(acetonitrile) copper(I) hexafluorophosphate in MeOH was added dropwise. The mixture was stirred for another 40 min followed by precipitation with 1 mL of MeOH and redispersion in 1 mL of toluene. For the $Cu^{+} \rightarrow Cd^{2+}$ exchange, 1 mL of the Cu-based NRs in toluene and 1 mL of ODE (previously degassed at 150 °C for 3 h) was heated to 250 °C. Then, 392 μL of TOP was added slowly, followed by dropwise addition of 46 mg of Cd(II) acetate in 375 μL of oleylamine. The solution was kept in 250 °C while stirring for 40 min, after which it was cooled to room temperature and the NRs were precipitated with 0.5 mL of toluene and 1 mL of MeOH and redispersed in toluene. This step was repeated either once or twice to further reduce the fraction of residual Cu in the Cd-exchanged NRs.

Elemental Analysis. Samples were prepared in a 25 mL volumetric flask, drying a known amount of toluene NR solution under nitrogen flow and digesting the dry residue overnight in 2.5 mL of aqua regia ($HCl:HNO_3$, 3:1 by volume). Prior to the measurement, the sample was diluted to a total volume of 25 mL with Millipore water and stirred by vortex for 10 s at 2400 rpm. Then, the sample was filtered using a PTFE membrane (0.45 μm pore size). Measurements were carried out with a ThermoFisher ICAP 6000 Duo inductively coupled plasma optical emission spectrometer. Three measurements were performed to obtain the final averaged value.

TEM and Optical Characterization. TEM images of the QDs were taken at 120 kV, using a transmission electron microscope (CM-120, Philips). UV−vis absorption spectra were measured using a UV−vis/NIR spectrophotometer (V-670, JASCO). PL spectra were measured using a custom-made orthogonal collection setup. The excitation was with a fiber coupled 405 nm LED Light Source (prizmatrix), collecting the fluorescence through a fiber, to measure the fluorescence spectrum with a USB4000 Ocean Optics spectrometer. QY measurements were conducted using an absolute quantum yield characterization system (Hamamatsu Quantaurus QY).

Biexciton Spectroscopy. Excitation pulses were generated by a frequency tripled Nd:YAG Q-switched laser oscillator pumping an optical parametric oscillator (OPO) (NT342/C/3/UVE, EKSPLA) with pulse durations of ∼5 ns at a repetition rate of 10 Hz. Excitation pulses at 450 nm were obtained from the OPO and focused into a 10 × 10 mm rectangular quartz cuvette (Starna Cells), containing a solution of a low concentration of QDs dispersed in toluene. Fluorescence signals were collected at a right-angle by a 0.4 NA objective. After spectral filtering by a dielectric long-pass filter, the signal was further passed through a monochromator (SpectraPro 2150i, Acton) for complete filtering of the laser pulses from the fluorescence. Time-resolved signals were measured by a photomultiplier tube (R10699, Hamamatsu Photonics, Hamamatsu City, Japan). Data was collected by a 600 MHz oscilloscope (WaveSurfer 62Xs, Teledyne LeCroy). Pulse energies were measured by a pyroelectric sensor (PE9-C, Ophir Optronics). The excitation beam area was measured using a high resolution CCD camera (DCU223M, Thorlabs), and the laser power density was calculated assuming a Gaussian beam profile. Power density values ranged from 0.03 J/cm^2 to 18 J/cm^2.

ASSOCIATED CONTENT

Supporting Information

The Supporting Information is available free of charge on the ACS Publications website at DOI: 10.1021/acs.chemmater.6b03332.

A more detailed account of the nanocrystal synthesis, ICP results, BX spectroscopy analysis, and CdSe/CdS NRs optical characterization (PDF)

AUTHOR INFORMATION

Corresponding Author

*(D.O.) E-mail: dan.oron@weizmann.ac.il.

Present Address

§(D.O.) Department of Physics of Complex Systems, Weizmann Institute of Science, Rehovot 7610001, Israel.

Author Contributions

N.M. performed the nanocrystals synthesis, EM characterization, and spectroscopic experiments. B.M.-G performed the

DOI: 10.1021/acs.chemmater.6b03332
Chem. Mater. 2016, 28, 7872−7877

cation exchange and related characterization. The work was conceived and supervised by D.O. and I.M. The manuscript was written by N.M. with significant contributions of all authors. All authors have given approval to the final version.

Funding

This work is funded by the Ministry of Science, Technology and Space of the state of Israel, the Ministero degli Affari Esteri e della Cooperazione Internazionale of Italy (IONX-NC4SOL), and by the Crown Photonics Center of the Weizmann Institute of Science. This project has also received funding from the European Union's Horizon 2020 research and innovation program under Grant Agreement No. 696656 (Graphene-Core1).

Notes

The authors declare no competing financial interest.

■ ACKNOWLEDGMENTS

The authors thank M. Kazes (WIS) for important contributions at the early stages of this work and for helpful discussions throughout it. F. Drago and G. La Rosa (IIT) are acknowledged for performing the ICP-OES measurements.

■ REFERENCES

(1) Jain, P. K.; Beberwyck, B. J.; Fong, L.-K.; Polking, M. J.; Alivisatos, a. P. Highly Luminescent Nanocrystals From Removal of Impurity Atoms Residual From Ion-Exchange Synthesis. *Angew. Chem., Int. Ed.* **2012**, *51*, 2387−2390.

(2) Son, D. H.; Hughes, S. M.; Yin, Y.; Alivisatos, A. P. Cation Exchange Reactions in Ionic Nanocrystals. *Science (Washington, DC, U. S.)* **2004**, *306*, 1009−1012.

(3) Luther, J. M.; Zheng, H.; Sadtler, B.; Alivisatos, a. P. Synthesis of PbS Nanorods and Other Ionic Nanocrystals of Complex Morphology by Sequential Cation Exchange Reactions. *J. Am. Chem. Soc.* **2009**, *131*, 16851−16857.

(4) Li, H.; Zanella, M.; Genovese, A.; Povia, M.; Falqui, A.; Giannini, C.; Manna, L. Sequential Cation Exchange in Nanocrystals: Preservation of Crystal Phase and Formation of Metastable Phases. *Nano Lett.* **2011**, *11*, 4964−4970.

(5) Robinson, R. D.; Sadtler, B.; Demchenko, D. O.; Erdonmez, C. K.; Wang, L.-W.; Alivisatos, a P. Spontaneous Superlattice Formation in Nanorods through Partial Cation Exchange. *Science* **2007**, *317*, 355−358.

(6) Casavola, M.; van Huis, M. A.; Bals, S.; Lambert, K.; Hens, Z.; Vanmaekelbergh, D. Anisotropic Cation Exchange in PbSe/CdSe Core/Shell Nanocrystals of Different Geometry. *Chem. Mater.* **2012**, *24*, 294−302.

(7) Sadtler, B.; Demchenko, D. O.; Zheng, H.; Hughes, S. M.; Merkle, M. G.; Dahmen, U.; Wang, L.; Alivisatos, a. P. Selective Facet Reactivity during Cation Exchange in Cadmium Sulfide Nanorods Selective Facet Reactivity during Cation Exchange in Cadmium Sulfide Nanorods. *J. Am. Chem. Soc.* **2009**, *131*, 5285−5293.

(8) Smith, A. M.; Nie, S. Bright and Compact Alloyed Quantum Dots with Broadly Tunable Near-Infrared Absorption and Fluorescence Spectra through Mercury Cation Exchange. *J. Am. Chem. Soc.* **2011**, *133*, 24−26.

(9) Justo, Y.; Sagar, L. K.; Flamee, S.; Zhao, Q.; Vantomme, A.; Hens, Z. Less Is More. Cation Exchange and the Chemistry of the Nanocrystal Surface. *ACS Nano* **2014**, *8*, 7948−7957.

(10) Tu, R.; Xie, Y.; Bertoni, G.; Lak, A.; Gaspari, R.; Rapallo, A.; Cavalli, A.; De Trizio, L.; Manna, L. Influence of the Ion Coordination Number on Cation Exchange Reactions with Copper Telluride Nanocrystals. *J. Am. Chem. Soc.* **2016**, *138*, 7082−7090.

(11) Jain, P. K.; Amirav, L.; Aloni, S.; Alivisatos, a. P. Nanoheterostructure Cation Exchange: Anionic Framework Conservation. *J. Am. Chem. Soc.* **2010**, *132*, 9997−9999.

(12) Li, H.; Brescia, R.; Povia, M.; Prato, M.; Bertoni, G.; Manna, L.; Moreels, I. Synthesis of Uniform Disk-Shaped Copper Telluride Nanocrystals and Cation Exchange to Cadmium Telluride Quantum Disks with Stable Red Emission. *J. Am. Chem. Soc.* **2013**, *135*, 12270−12278.

(13) Avidan, A.; Oron, D. Large Blue Shift of the Biexciton State in Tellurium Doped CdSe Colloidal Quantum Dots. *Nano Lett.* **2008**, *8*, 2384−2387.

(14) Avidan, A.; Deutsch, Z.; Oron, D. Interactions of Bound Excitons in Doped Core/shell Quantum Dot Heterostructures. *Phys. Rev. B: Condens. Matter Mater. Phys.* **2010**, *82*, 165332.

(15) Zhang, L.; Lin, Z.; Luo, J.-W.; Franceschetti, A. The Birth of a Type-II Nanostructure: Carrier Localization and Optical Properties of Isoelectronically Doped CdSe:Te Nanocrystals. *ACS Nano* **2012**, *6*, 8325−8334.

(16) Li, H.; Brescia, R.; Krahne, R.; Bertoni, G.; Alcocer, M. J. P.; D'Andrea, C.; Scotognella, F.; Tassone, F.; Zanella, M.; De Giorgi, M.; Manna, L. Blue-UV-Emitting ZnSe(Dot)/ZnS(Rod) Core/shell Nanocrystals Prepared from CdSe/CdS Nanocrystals by Sequential Cation Exchange. *ACS Nano* **2012**, *6*, 1637−1647.

(17) Oron, D.; Kazes, M.; Banin, U. Multiexcitons in Type-II Colloidal Semiconductor Quantum Dots. *Phys. Rev. B: Condens. Matter Mater. Phys.* **2007**, *75*, 035330.

(18) Sitt, A.; Della Sala, F.; Menagen, G.; Banin, U. Multiexciton Engineering in Seeded Core/shell Nanorods: Transfer from Type-I to Quasi-Type-II Regimes. *Nano Lett.* **2009**, *9*, 3470−3476.

(19) Bae, W. K.; Padilha, L. a; Park, Y.-S.; McDaniel, H.; Robel, I.; Pietryga, J. M.; Klimov, V. I. Controlled Alloying of the Core-Shell Interface in CdSe/CdS Quantum Dots for Suppression of Auger Recombination. *ACS Nano* **2013**, *7*, 3411−3419.

(20) Li, J. J.; Wang, Y. A.; Guo, W.; Keay, J. C.; Mishima, T. D.; Johnson, M. B.; Peng, X. Large-Scale Synthesis of Nearly Monodisperse CdSe/CdS Core/shell Nanocrystals Using Air-Stable Reagents via Successive Ion Layer Adsorption and Reaction. *J. Am. Chem. Soc.* **2003**, *125*, 12567−12575.

(21) Van Embden, J.; Jasieniak, J.; Mulvaney, P. Mapping the Optical Properties of CdSe/CdS Heterostructure Nanocrystals: The Effects of Core Size and Shell Thickness. *J. Am. Chem. Soc.* **2009**, *131*, 14299−14309.

(22) Christodoulou, S.; Vaccaro, G.; Pinchetti, V.; De Donato, F.; Grim, J. Q.; Casu, a.; Genovese, a.; Vicidomini, G.; Diaspro, a.; Brovelli, S.; Manna, L.; Moreels, I. Synthesis of Highly Luminescent Wurtzite CdSe/CdS Giant-Shell Nanocrystals Using a Fast Continuous Injection Route. *J. Mater. Chem. C* **2014**, *2*, 3439.

(23) Angeloni, I.; Raja, W.; Brescia, R.; Polovitsyn, A.; De Donato, F.; Canepa, M.; Bertoni, G.; Proietti Zaccaria, R.; Moreels, I. Disentangling the Role of Shape, Ligands, and Dielectric Constants in the Absorption Properties of Colloidal CdSe/CdS Nanocrystals. *ACS Photonics* **2016**, *3*, 58−67.

DOI: 10.1021/acs.chemmater.6b03332
Chem. Mater. 2016, 28, 7872−7877